Published in final edited form as:

Mol Cancer Res. 2019 March ; 17(3): 697–708. doi:10.1158/1541-7786.MCR-18-0666.

Growth Factor–Independent 1 Is a Tumor Suppressor Gene in Colorectal Cancer

Min-Shan Chen[1], **Yuan-Hung Lo**[1], **Xi Chen**[2], **Christopher S. Williams**[3], **Jessica M. Donnelly**[4], **Zachary K. Criss II**[5], **Shreena Patel**[6], **Joann M. Butkus**[4,7,8], **Julien Dubrulle**[9], **Milton J. Finegold**[10], **Noah F. Shroyer**[1,4,5]

[1]Integrative Molecular and Biomedical Sciences Graduate Program, Baylor College of Medicine, Houston, Texas.

[2]Department of Public Health Sciences, University of Miami, Miami, Florida.

[3]Department of Medicine, Division of Gastroenterology, Hepatology, and Nutrition, Vanderbilt University, Nashville, Tennessee.

[4]Department of Medicine, Section of Gastroenterology and Hepatology, Baylor College of Medicine, Houston, Texas.

[5]Translational Biology and Molecular Medicine Graduate Program, Baylor College of Medicine, Houston, Texas.

[6]Department of Pediatrics, Section of Gastroenterology, Hepatology, and Nutrition, Baylor College of Medicine, Houston, Texas.

[7]Summer Undergraduate Research Training Program, Baylor College of Medicine, Houston Texas.

[8]Susquehanna University, Selinsgrove, Pennsylvania.

[9]Integrated Microscopy Core, Baylor College of Medicine, Houston, Texas.

[10]Department of Pathology and Immunology, Baylor College of Medicine, Houston, Texas.

Corresponding Author: Noah F. Shroyer, Baylor College of Medicine, Houston, TX 77030. Phone: 713-798-8693; Noah.shroyer@bcm.edu.

Authors' Contributions

Conception and design: M.-S. Chen, Y.-H. Lo, N.F. Shroyer

Development of methodology: M.-S. Chen, N.F. Shroyer

Acquisition of data (provided animals, acquired and managed patients, provided facilities, etc.): M.-S. Chen, Z.K. Criss II, S. Patel, J.M. Butkus, N.F. Shroyer

Analysis and interpretation of data (e.g., statistical analysis, biostatistics, computational analysis): M.-S. Chen, X. Chen, Z.K. Criss II, S. Patel, J. Dubrulle, M.J. Finegold, N.F. Shroyer

Writing, review, and/or revision of the manuscript: M.-S. Chen, C.S. Williams, J.M. Donnelly, Z.K. Criss II, S. Patel, J.M. Butkus, N.F. Shroyer

Administrative, technical, or material support (i.e., reporting or organizing data, constructing databases): M.-S. Chen, J.M. Butkus, N.F. Shroyer

Study supervision: N.F. Shroyer

Note: Supplementary data for this article are available at Molecular Cancer Research Online (http://mcr.aacrjournals.org/).

Disclosure of Potential Conflicts of Interest

No potential conflicts of interest were disclosed.

The costs of publication of this article were defrayed in part by the payment of page charges. This article must therefore be hereby marked *advertisement* in accordance with 18 U.S.C. Section 1734 solely to indicate this fact.

Abstract

Colorectal cancer is the third most common cancer and the third leading cause of cancer death in the United States. Growth factor–independent 1 (GFI1) is a zinc finger transcriptional repressor responsible for controlling secretory cell differentiation in the small intestine and colon. GFI1 plays a significant role in the development of human malignancies, including leukemia, lung cancer, and prostate cancer. However, the role of GFI1 in colorectal cancer progression is largely unknown. Our results demonstrate that RNA and protein expression of GFI1 are reduced in advanced-stage nonmucinous colorectal cancer. Subcutaneous tumor xenograft models demonstrated that the reexpression of GFI1 in 4 different human colorectal cancer cell lines inhibits tumor growth. To further investigate the role of Gfi1 in *de novo* colorectal tumorigenesis, we developed transgenic mice harboring a deletion of Gfi1 in the colon driven by CDX2-cre ($Gfi1^{F/F}$; CDX2-cre) and crossed them with $Apc^{Min/+}$ mice ($Apc^{Min/+}$; $Gfi1^{F/F}$; CDX2-cre). Loss of Gfi1 significantly increased the total number of colorectal adenomas compared with littermate controls with an APC mutation alone. Furthermore, we found that compound ($Apc^{Min/+}$; $Gfi1^{F/F}$; CDX2-cre) mice develop larger adenomas, invasive carcinoma, as well as hyperplastic lesions expressing the neuroendocrine marker chromogranin A, a feature that has not been previously described in APC-mutant tumors in mice. Collectively, these results demonstrate that *GFI1* acts as a tumor suppressor gene in colorectal cancer, where deficiency of Gfi1 promotes malignancy in the colon.

Implications: These findings reveal that GFI1 functions as a tumor suppressor gene in colorectal tumorigenesis.

Introduction

Colorectal cancer is the third most commonly diagnosed cancer in the world, with approximately 1.4 million new cases diagnosed every year. In 2016, colorectal cancer was responsible for 8% of all new cancers and the third leading cause of cancer mortality in the United States (1). Unlike many other cancers, colorectal cancer progression is preventable and when detected early is associated with a good long-term prognosis (2). The 5-year survival rate is up to 90% when diagnosed with stage I or ll colorectal cancer, whereas the 5-year survival rate drops to 12% for those who were diagnosed with metastatic colorectal cancer (3). The transformation from benign adenoma to malignant carcinoma is estimated to take 7 to 10 years (4). This gap is what allows for early detection and the prevention of death.

Transcription factors are commonly deregulated in the pathogenesis of human cancers; these transcription factors control oncogenic signaling pathways leading to tumor initiation and progression as well as metastasis. Targeting these transcription factors holds tremendous therapeutic potential for cancer treatment (5). Growth factor–independent 1 (GFI1) is a zinc finger (ZNF) transcriptional repressor responsible for controlling hematopoietic stem cell quiescence, myeloid and lymphoid differentiation, and lymphocyte development and function (6–13). Outside of the hematopoietic system, GFI1 is required for secretory cell differentiation in the small intestine and colon as well as pulmonary neuroendocrine cell differentiation (14–16). GFI1 regulates several transcriptional circuits whose dysregulation leads to malignancies such as leukemia, lung cancer, and prostate cancer (17–20). However,

whether molecular alteration of *GFI1* is associated with colorectal cancer progression is still largely unknown. Genome sequencing analysis from The Cancer Genome Atlas suggested that *GFI1* expression is associated with less aggressive disease and better outcome. Thus, GFI1 may play a role in stalling tumor progression and metastasis in colorectal cancer (21). Here, we investigate whether dysregulation of GFI1 expression contributes to colorectal cancer tumorigenesis. For this study, we generated GFI1 overexpressing colorectal cancer cells and colon-specific knockout mice to examine the effect of manipulating GFI1 expression on colorectal cancer progression. Our results show *GFI1* RNA and protein levels are lost at advanced stages of human colorectal cancer. Reexpression of GFI1 in human colorectal cancer cell lines inhibits tumor growth in a subcutaneous tumor xenograft model. Loss of GFI1 in the colon accelerates the progression of malignancy in $Apc^{min/+}$ mice, promoting the formation of both high-grade adenomas and carcinoid-like lesions. Thus, our results indicate that GFI1 is a putative tumor suppressor in colorectal cancer.

Materials and Methods

Cell culture

The human colorectal cancer cell line HCT116, SW480, DLD1 and LOVO, as well as the human embryonic kidney cell lines HEK-293T were purchased from ATCC. All cells were grown in RPMI (Corning, 10–040-CV) supplemented with 10% fetal bovine serum (Bioexpress, S1200–500), and penicillin and streptomycin (Lonza, 17–602E). The doxycycline-inducible pINDUCER HCT116, SW480, DLD1, and LOVO cell lines were maintained in the same condition with tetracycline-free fetal bovine serum (Corning, #35–075-CV) and periodically selected by supplemental 500 μg/mL G418 (Sigma, #A1720).

Generation of doxycycline-inducible cell lines

The pENTR-GFI1 plasmid (Addgene #16168) was obtained from Addgene and cloned into pINDUCER20-Neo (22) using the Gateway Cloning Technology (Invitrogen). The resulting pINDU-CER20-GFI1-Neo plasmid was verified by DNA sequencing (BCM, sequence core). Virus was generated by transfection of 293T cells grown to 70% confluence in a 6-cm tissue culture plate with 2.25 μg envelope plasmid, pCMV-VSV-G (Addgene #8454) and 0.25 μg packaging plasmid, psPAX2 (Addgene #12260) and 2.5 μg pINDUCER20-GFI1-Neo plasmid or control plasmid pINDUCER20-Neo using Lipofectamine 2000 (Invitrogen) following the manufacturer's transfection protocol. Eighteen hours after transfection, the media in each well were replaced with fresh media. After 48 hours of viral production, virus-containing media were collected, pooled, filtered through a 0.45-μm poly-vinylidene difluoride membrane (Millex), and added to human colorectal cancer cell lines at 60% confluence in 10-cm tissue culture dishes (Corning). Infection was allowed to proceed for overnight, and then the media were replaced. After a 72-hour recovery period, infected cells were selected with 500 μg/mL G418 (Sigma, #A1720).

Western blot

Cell lysates of the treated cells were isolated by incubation with RIPA buffer, containing 150 mmol/L NaCl, 1 mmol/L EDTA pH 8.0, 25 mmol/L Tris, 0.1% SDS, 0.5% sodium deoxycholate, 1% NP-40, phosphatase inhibitor cocktails (Sigma, P5726 and P0044) and the

protease inhibitors cocktail (Calbiochem, #539134). Cell lysates were separated on acrylamide gels, transferred to a PVDF membrane (Bio-Rad), and probed with the Gfi1 antibody (1:1000, Santa Cruz Biotechnology, sc8558) and tubulin antibody (1: 100, DSHB, 6G7). Bands were visualized by a chemiluminescence-based detection method (Fisher/Pierce) that used horseradish peroxidase–conjugated secondary antibodies (Cell Signaling Technology, #7076 and Santa Cruz Biotechnology, sc-2056). For colon tissues, frozen tissues were homogenized in RIPA buffer and sonicated for 10 seconds. Protein concentration was measured by the BCA kit (Thermo Fisher, #23225).

Mice

NOD.Cg-*Prkdc*^{scid} *IL2rg*^{tm1Wjl} (NSG) immunodeficient mice (#00557) were obtained from The Jackson Laboratory. For xenograft studies, male NSG mice were randomly divided into experimental groups. Mice were subcutaneously injected with doxycycline-inducible HCT116, SW480, DLD1, or LOVO cells (2×10^6 cells in a 100 μL serum-free RPMI-1640 with 50% matrigel). Mice were fed doxycycline diet (625 mg/kg, Envigo Teklad) 3 days before inoculation of HCT116, SW480, DLD1, or LOVO cells. Tumor volume (mm^3) was calculated using the following formula: tumor volume (mm^3) = length (mm) × width^2 (mm^2) × 0.5. Apc$^{Min/+}$ mice were purchased from The Jackson Laboratory (#002020). CDX2-cre mice (23) were obtained from Dr. Jason Heaney at Baylor College of Medicine. Gfi1$^{F/F}$ mice (10) were obtained from Dr. Jinfang Zhu at National Institutes of Health. All mouse studies were approved by the Institutional Animal Care and Use Committee (IACUC).

Analysis of cell cycle by flow cytometry

GFI1-expressing cells and control cells were treated with 1 μg/mL doxycycline to induce Gfi1 expression for 48 hours. Cells were trypsinized and fixed in cold 70% ethanol for 2 hours and then stained with 10 μL propidium iodide (PI) solution (0.5 mg/mL PI and 0.125% RNaseA; Sigma) at room temperature for 15 minutes. Approximately 10,000/sample cells were analyzed using LSRFortessa (Becton Dickinson).

Tissue staining

Colon and tumors were fixed with 4% paraformaldehyde (PFA) at 4°C overnight, washed with PBS, and then transferred to 70% ethanol for paraffin-embedding. Tissues were sectioned at 5-μm thickness. For IHC staining, paraffin-embedded sections were deparaffinized and rehydrated before staining. For IHC, antigen retrieval was achieved in sodium citrate buffer (10 mmol/L sodium citrate pH 6.0). Slides were incubated in 3% H_2O_2 solution in methanol at room temperature for 10 minutes to block endogenous peroxidase activity. After washing, slides were blocked in avidin/biotin solution (Vector Laboratories, SP2001) for 30 minutes and then in 5% normal goat or donkey serum in PBST at room temperature for 1 hour. After blocking, slides were incubated with primary antibody at 4°C overnight. Slides were washed by PBST at room temperature for 5 minutes 3 times and incubated with secondary antibody at room temperature for 0.5 hours. Slides were washed by PBST and then ABC reagent applied (Vector Laboratories, PK-6101) for 0.5 hours. Slides were washed by PBST and signals were detected by DAB (Vector Laboratories, SK-4100). For immunofluorescent staining, deparaffinization and rehydration procedures were as described above. Slides were blocked with 5% serum at room temperature for 1 hour

or MOM reagent if a mouse antibody was used (Vector Laboratories, PK-2200). Primary antibody was diluted in 5% serum in PBST and incubated with tissues at 4°C for overnight. Slides were washed by PBST (at room temperature for 3 minutes for 3 times) and incubated with secondary antibody at room temperature for 1 hour. After 3 washes, slides were stained with DAPI (Thermo Fisher, #62248) at room temperature for 10 minutes. Slides were washed twice with PBS. Slides were mounted with mounting solution (Vector Laboratories, H-1000). The following antibodies were used: goat Gfi1 (1:100 Santa Cruz Biotechnology, sc-8558), rabbit Ki67 (1:1,000 Leica, NCL-Ki67p), rabbit caspase-3 (1:500 Cell Signaling Technology 9661s), rabbit phospho-histone3 (1:1,000 Cell Signaling Technology 3377s), biotinylated rabbit anti-goat IgG antibody (1:200 Vector Laboratories, BA-5000), biotinylated goat anti-rabbit IgG antibody (1:200 Vector Laboratories, BA-1000), mouse PCNA (1:1,000, Cell Signaling Technology, #2586), mouse E-cadherin (1:250 Abcam, ab76055), rabbit beta-catenin (1:500 Santa Cruz Biotechnology, sc-7199), mouse CD45 (1:50, DSHB, H5A5-s), rabbit chromogranin A (1:1,000, immunostar, 20085). For goblet cell staining, slides were stained with Alcian blue (Thermo Fisher, 88043) following the manufacturer's protocol.

Protein analysis of colorectal cancer tissue array

Colon cancer tissue microarray was obtained from the Pathology Core at Baylor College of Medicine. To determine the GFI1 immunostaining score, we used the scoring system by Klein and colleagues (24). In brief, this score was established as: each sample was scored twice—(i) for the percentage of labeled colonic epithelial cells (0, absence of labeling; 1, <30%; 2, 30%–60%; 3, >60% of colonic epithelial cells are labeled); and (ii) for the intensity of the immunostaining (0, no staining; 1, weak; 2, mild; 3, strong staining). Multiplication of both scores allowed the final quotation ranging from 0 to 9. Fifty-two nonmucinous colorectal cancer samples, 11 mucinous colorectal cancer samples, and 7 adjacent normal colon samples were analyzed.

RNA analysis of colorectal cancer tumors

To determine if *GFI1* expression was significantly different between normal adjacent colon, analysis of the combined Moffit Cancer Center (MCC) and Vanderbilt Medical Center (VMC) colon tumor expression array data set (10, normal samples; 6, adenomas; 33, stage I; 76, stage 2; 82, stage 3; and 59, stage 4; for combined total of 250 colorectal cancer samples) was performed (25). The expression array data have been deposited, and the GEO accession number is GSE17538. Complete minimum information about a microarray experiment–compliant data sets for analysis is available (http://www.ncbi.nlm.nih.gov/geo/query/acc.cgi?acc=GSE17538). The microarray data were normalized using Robust Multichip Averaging algorithm implemented in Bioconductor package Affy. Log2 transformed data were used for downstream analyses. The Wilcoxon and Kruskal–Wallis rank sum tests were used to test for significance between each stage and the normal adjacent tissue.

Survival analysis

Colorectal cancer patients from VMC/MCC with *GFI1* high expression were defined as having greater than median expression of *GFI1* and were compared with the low-expression

group (less than the median expression value). Kaplan–Meier analysis was performed, comparing patients with high *GFI1* expression (red line) to low *GFI1* expression (blue line). Although not achieving statistical significance, patients with high *GFI1* expression had better relapse-free survival than patients with low *GFI1* expression (log-rank test $P = 0.1692$).

Apoptosis assay

Cells were washed with PBS, trypsinized, and resuspended in the Annexin V staining buffer (BioLegend, #42201) at concentration of 1×10^6 cells/mL. Cell suspensions (100 μL) were transferred to 5 mL flow tube and stained with 5 μL Annexin V–FITC (BioLegend, #640906) and 10 μL PI solution (0.5 mg/mL) for 15 minutes at room temperature in the dark. Binding buffer (400 μL) was added to each tube, and stained cells were analyzed by FACS analyzer LSRFortessa (Becton Dickinson).

Quantitative image analysis of IHC stains

Images were analyzed in MATLAB using a custom-made script. Cells were identified from the grayscale-converted, complemented RGB images by applying an extended maxima transform function followed by common morphologic operations. Caspase-3 or phosphor-Histone H3 DAB-positive cells were identified by pixel color classification after converting the RGB image in L*a*b color space. The accuracy of the algorithm was assessed by visual inspection of the segmentation process.

Statistical analysis

All analyses were performed using GraphPad Prism version 7.0d (GraphPad Software). Student *t* test was used for the comparison of 2 groups. Statistical comparisons between multiple groups were analyzed using the one-way ANOVA. Significance was taken as $P < 0.05$.

Results

GFI1 messenger RNA and protein levels are silenced in the majority of human colon tumors

Previous studies suggested that *GFI1* mRNA expression is associated with less aggressive colorectal cancers (21). To further examine the role of GFI1 in human colon tumorigenesis and metastasis, we analyzed *GFI1* mRNA expression in samples representing each stage of colorectal cancer development. We found *GFI1* transcript levels were significantly decreased in all stages of colorectal cancer compared with those in normal colon or benign adenomas (normal vs. all stages, *P* value = 1.267e–5, stage I vs. stage IV, *P* value = 0.002; Fig. 1A). RNA data suggested that *GFI1* loss occurs later in the progression to tumorigenesis, as there was no significant difference in expression between normal colonic tissue and benign adenomas (Fig. 1A). Analysis of survival data showed that colorectal cancer patients with tumors that had high expression of *GFI1* had a better survival rate compared with colorectal cancer patients with low expression of *GFI1* (Fig. 1B). To further examine the protein expression level of GFI1 in human colorectal tumors, we analyzed an array of colonic tissue, including 87 tumor cases obtained from the Pathology Core at Baylor College of Medicine.

Specificity of the GFI1 antibody was confirmed by peptide competition assay (Supplementary Fig. S1A). GFI1 protein levels were significantly decreased in all stages of colorectal cancer compared with normal colon (normal vs. all stages, *P* value < 0.0001, normal vs. stage I, *P* value = 0.028, normal vs. stage II, *P* value = 0.0002, normal vs. stage III, *P* value = 0.0002, normal vs. stage IV, *P* value = 0.0011; Fig. 1C). We also observed staining of scattered cells in the lamina propria, consistent with the expression of GFI1 in bone marrow stromal cells and hematopoietic cells such as neutrophils, as previously reported (26). CD45 immunostaining confirmed that GFI1-positive cells in the lamina propria are hematopoietic cells (Supplementary Fig. S1B). We noted that 6 of 7 (85%) mucinous tumors retained GFI1 expression with higher cytoplasmic and nuclear staining compared with nonmucinous adenocarcinoma (normal vs. nonmucinous, *P* value < 0.0001, normal vs. mucinous, *P* value = 0.3506, nonmucinous vs. mucinous, *P* value = 0.0002); Fig. 1D and E), indicating that different mechanisms may control GFI1 expression in mucinous colorectal cancers compared with the more common nonmucinous adenocarcinoma. These results confirm the mRNA expression data and point to a potential role for GFI1 as a tumor suppressor in the colon.

GFI1 expression has moderate effects on growth and apoptosis in colorectal cancer cells *in vitro*

Our results showed expression of GFI1 is reduced in tumors from colorectal cancer patients (Fig. 1C and D), and furthermore GFI1 is undetectable in human colorectal cancer cell lines (Fig. 2B and C). To investigate the effect of GFI1 reexpression on colorectal cancer progression, we generated human colorectal cancer cell lines that express GFI1 in a doxycycline-inducible manner (Fig. 2A). The human colorectal cancer cell lines HCT116, SW480, DLD1, and LOVO were engineered to stably express doxycycline-inducible GFI1 protein and are referred to as HCT116-hGFI1, SW480-hGFI1, DLD1-hGFI1, and LOVO-hGFI1, respectively. Control cell lines were transfected with an empty vector and were designated HCT116-con, SW480-con, DLD1-con, and LOVO-con. GFI1 protein was detectable in the HCT116-hGFI1, SW480-hGFI1, DLD1-hGFI1, and LOVO-hGFI1 cells after 48 hours of induction using immunoblot (Fig. 2B) and immunostaining (Fig. 2C). Next, to examine whether reexpression of GFI1 affects the cell cycle, flow cytometry was performed using PI DNA staining of GFI1-expressing or control colorectal cancer cells 48 hours after induction (Supplementary Fig. S2A). HCT116-hGFI1, SW480-hGFI1 showed a decrease in the number of cells in the G_0–G_1 phase and accumulation of cells in the S and G_2–M phases compared with controls. However, no significant differences were observed in any phase of the cell cycles in the DLD1-hGFI1 and LOVO-hGFI1 cell lines compared with controls. Furthermore, assessment of apoptosis by flow cytometry using Annexin V/PI staining showed no difference between GFI1-expressing and control colorectal cancer cells 72 hours after induction (Supplementary Fig. S2B). These results indicated that reexpression of GFI1 has a modest effect on cell cycle and no effect on apoptosis *in vitro*.

GFI1 overexpression impairs growth of human colorectal cancer xenografts

To test whether reexpression of GFI1 inhibits cancer cell growth *in vivo*, we subcutaneously injected Gfi1-expressing cells (HCT116-hGFI1, SW480-hGFI1, DLD1-hGFI1, and LOVO-hGFI1) and control cells (HCT116-con, SW480-con, DLD1-con, and LOVO-con) into the

right and left rear flanks, respectively, of immunodeficient mice (Fig. 2D). Mice were fed with doxycycline chow 3 days before and continuously after cancer cell transplantation to induce GFI1 expression (Fig. 2E). Tumor size and body weight were measured twice a week for 4 weeks. We found that in all 4 colorectal cancer cell lines, GFI1 expression significantly reduced the initiation of human colorectal cancer growth (Fig. 2F–I). Xenograft tissue was collected after 4 weeks of growth and analyzed histologically. IHC staining showed GFI1 expression in LOVO cell-derived xenograft after induction by doxycycline (Fig. 2J). Analysis of xenograft proliferation by immunostaining with the metaphase marker phospho-Histone 3 showed that GFI1 expression reduced proliferation of all 4 colorectal cancer cell lines compared with controls, with statistically significant results observed in DLD1 and SW480 cells (Fig. 3A and B). Assessment of xenograft apoptosis by immunostaining for cleaved-caspase-3 showed that GFI1 expression increased apoptosis in all 4 colorectal cancer cell lines compared with controls, with statistically significant results observed in HCT116, LOVO, and SW480 cells (Fig. 3C and D). Together, these results indicate that GFI1 inhibits tumor cell proliferation and increases tumor cell apoptosis in subcutaneous tumor xenografts in mice.

Loss of Gfi1 in distal intestine is associated with colon tumorigenesis

To investigate the effect of *Gfi1* deficiency on colorectal adenoma formation and progression, we crossed mice with transgenic cre-mediated deletion of *Gfi1* in the intestine ($Gfi1^{F/F}$; CDX2-cre mice) with $Apc^{Min/+}$ mice, the best-studied model of *de novo* colon tumorigenesis. In adult CDX2-cre mice, Cre activity is limited to the colon and distal ileum, which we confirmed by crossing CDX2-cre with reporter Rosa26-tdTomato mice (Supplementary Fig. S3). $Apc^{Min/+}$; $Gfi1^{F/F}$; CDX2-cre mice developed significantly larger and more tumors in the rectum and colon at age 4 to 5 months than littermates retaining *Gfi1* ($Apc^{Min/+}$; $Gfi1^{F/+}$; CDX2-cre and $Apc^{Min/+}$; Fig. 4A and B). In contrast to control $Apc^{Min/+}$ mice, which develop few colonic tumors, $Apc^{Min/+}$; $Gfi1^{F/F}$; CDX2-cre mice had a >5-fold increase in colorectal adenoma multiplicity (average number of colorectal adenomas per mouse: 29 vs. 5; Fig. 4C). Colorectal adenomas from $Apc^{Min/+}$; $Gfi1^{F/F}$; CDX2-cre mice were also larger than in $Apc^{Min/+}$ mice, with a 4-fold increase in the number of large tumors (>4 mm) and 13-fold increase in the number of medium-sized tumors (between 2 and 4 mm; Fig. 4D). PCR analysis confirmed the Cre-mediated deletion of the *Gfi1* allele (exon 4 and exon5), indicating that the larger tumors arose from Gfi1-mutant tissue (Fig. 4E). Immunoblotting further indicated Gfi1 was lost in Gfi1 knockout tissues (Fig. 4F). Histologic analysis confirmed the increased tumor burden, and that the increased tumor size was due to expansion in tumor cells and not cystic structures or inflammatory infiltrate (Fig. 5A). $Apc^{Min/+}$; $Gfi1^{F/F}$; CDX2-cre knockout mice developed both highly proliferating adenomas and invasive carcinomas that had penetrated below the muscularis mucosa, which were not seen in control, $Apc^{Min/+}$ mice (Fig. 5B). We have quantified proliferative cells in these adenomas and found a higher percentage of tumor cells positively stained for Ki-67 in $Apc^{Min/+}$; $Gfi1^{F/F}$; CDX2-cre mice compared with control mice (Fig. 5C). Homozygous deletion of *Gfi1* in mice has been shown to affect secretory cell differentiation in the intestine with reduced numbers of goblet and Paneth cells and the increased numbers of enteroendocrine cells (15). We characterized mucous-secreting cells using Alcian blue staining of acidic mucins, which are normally restricted to pregoblet and goblet cells in the

colon. In tumors from both $Apc^{Min/+}$; $Gfi1^{F/F}$; CDX2-cre and $Apc^{Min/+}$ mice, we observed a reduction in mucous-secreting goblet cells (Supplementary Fig. S4A and S4B). Cells within the adenomas stained for Ki67 and PCNA, indicating that they were actively proliferating in *Gfi1* knockout and control mice (Supplementary Fig. S4A). Consistent with their reduced secretory cell differentiation (27), $Apc^{Min/+}$ mice developed adenomas without enteroendocrine features. In contrast, we found increased expression of the enteroendocrine cell marker, chromogranin A (CgA), in *Gfi1-mutant* mice (Fig. 5D; Supplementary Fig. S4D). We observed 3 different patterns of CgA^+ cell staining in $Apc^{Min/+}$; $Gfi1^{F/F}$; CDX2-cre mice: first, we observed increased numbers of CgA^+ cells in the normal-appearing glands and surface epithelium of the colon, similar to what we observed in nontumor-bearing $Gfi1^{F/F}$; CDX2-cre (Fig. 5D); second, we observed that CgA^+ cells were reduced in hyperproliferating adenomatous tissues from polyps and areas of carcinoma (Supplementary Fig. S4A and S4C); third, we observed clusters of CgA^+ cells in scattered lesions that arose in areas with hyperplastic crypts in the colon of $Apc^{Min/+}$; $Gfi1^{F/F}$; CDX2-cre mice (Fig. 5D; Supplementary Fig. S4C). These CgA^+ cell clusters generally did not express PCNA (<0.01% proliferation, PNCA labeling index, Supplementary Fig. S4E), suggesting that they are well-differentiated and slow-growing pseudotumor lesions. RT-qPCR analysis showed increased expression of *chromogranin A* and decreased expression of the goblet cell marker *Muc2* in *Gfi1* knockout tumors compared with control tumors (Supplementary Fig. S4B). Taken together, these results indicated that *Gfi1* deficiency greatly promotes tumor malignancy and formation of hyperplastic lesions with neuroendocrine features in the colon and rectum.

Discussion

Colorectal cancer is a highly heterogeneous disease caused by different molecular pathways with diverse morphologic features, clinical outcomes, and response to cancer therapy. The dysregulation of several transcription factors is known to contribute to intestinal tumorigenesis (28). GFI1 is a ZNF transcriptional repressor implicated in diverse developmental contexts (29). Several studies have suggested that ZNF transcription factors act as double-edged sword during tumorigenesis in different cancer types (30). GFI1 is critical to several transcriptional circuits whose dysregulation results in oncogenesis in the hematopoietic system, lung cancer, prostate cancer, and medulloblastoma (17–19, 31, 32). RNA expression in colorectal cancers compared to tumor stage, lymph node status, distant metastasis, and vascular invasion at the time of surgery has shown that higher expression of *GFI1* was associated with less tumor aggressiveness (21). In the present study, we found the expression of GFI1 is progressively lost in human colorectal cancer tissues. Moreover, we found that colorectal cancer patients with tumors expressing lower levels of *GFI1* had a poor survival rate. Consistent with these findings, in human colon cancer cell lines, we found that expression of GFI1 inhibits growth of subcutaneous xenograft tumors. Furthermore, we demonstrated that deletion of *Gfi1* in the intestinal epithelium promoted colorectal malignancy with an increased number of tumors and formation of more advanced adenocarcinomas in the distal colon and rectum compared with controls. Recently, Xing and colleagues reported that GFI1 downregulation promotes inflammation-induced colorectal cancer metastasis through the activation of inflammatory signaling that enhances the

invasive behavior of colorectal cancer cells (33). Together, our study and that of Xing and colleagues support GFI1's function as a tumor suppressor in colorectal cancer.

The molecular mechanisms that result in loss of GFI1 protein in advanced colorectal cancer (Fig. 1) are not well understood, and may occur by multiple mechanisms. *GFI1* is not subject to frequent point mutation or copy-number variation as reported in the COSMIC or ONCOMINE databases. Instead, we hypothesize that GFI1 expression is regulated by epigenetic mechanisms, such as DNA methylation or chromatin remodeling. Previous studies suggested that the expression of *Gfi1* could be regulated through a polycomb repressive complex 2 (PRC2)–dependent mechanism. PRC2 is an important chromatin modifier involved in the maintenance of transcriptional silencing by inducing mono, di-, and trimethylation of histone 3 at lysine 27 (H3K27me3; ref. 34). EZH2, a member of the PRC2 genes, is upregulated and correlated with poor prognosis in human CRCs (35, 36). In medulloblastoma, ChIP-seq analysis showed that EZH2 transcriptionally suppresses *Gfi1* directly, resulting in the inhibition of tumor growth (32). In addition, the expression of GFI1 could be regulated by components within the tumor microenvironment. Previous studies suggested that immune cell cytokines, such as IL1α, TGFβ, or IFNγ could contribute to GFI1 deregulation, thereby changing cancer cell behaviors (33). Finally, in the intestinal epithelium, our previous studies showed that *Gfi1* is a direct target of ATOH1, a master transcription factor that controls intestinal secretory cell fate determination (15, 37). In CRCs, ATOH1 functions as a colorectal cancer tumor suppressor (38). The expression of *ATOH1* is silenced due to either CpG island hypermethylation or deletion. Thus, downregulation of GFI1 might be due to loss of ATOH1 in CRCs (38). Future studies are needed to determine the mechanisms that control GFI1 stability and cofactor interactions in colorectal cancer tumorigenesis.

Mucinous colorectal cancer represents a distinct clinical and histopathologic subtype of colorectal cancer, and is found in 10% to 15% of patients with colorectal cancer. Mucinous colorectal cancer is associated with rapid disease progression and poor prognosis (39). It has been shown that mucinous colorectal cancer has different molecular alterations and genetic subtypes, when compared with nonmucinous colorectal cancer (40). Mucinous colorectal cancer shows more frequent microsatellite instability and oncogenic KRAS, BRAF, and PIK3CA mutations than nonmucinous colorectal cancer (41, 42). In this study, we found that *GFI1* expression is nearly absent in nonmucinous colorectal cancer, where it functions as a tumor suppressor; however, GFI1 is highly expressed in mucinous colorectal cancer (Fig. 1), suggesting that it must have distinct functions in mucinous colorectal cancer compared with nonmucinous colorectal adenomas and adenocarcinomas.

Carcinoids/gastrointestinal neuroendocrine tumors are composed of hormone-producing endocrine-like cells (43). These neuroendocrine tumors often release hormones into the blood-stream where they affect the function of other parts of the digestive system and a variety of other organ processes. A previous study suggested that overexpression of gastrointestinal hormones (gastrin) can drive formation of gastrointestinal tumors (44). It is possible that overexpression of hormones from carcinoid-like lesions in *Gfi1* knockout mice enhanced the formation and progression of colorectal adenomas in the context of *Apc* mutation. Canonical Wnt/β-catenin signaling is essential for the maintenance of intestinal

stem cells and secretory cell differentiation (45, 46). Within secretory progenitors, GFI1 promotes goblet and Paneth cell fate by repressing *Neurog3* expression (14, 15). Previous work indicated that Neurog3^{+} early precursors of enteroendocrine cells can respond to hyperactivation of β-catenin by developing serotonin-expressing adenomas in the small intestine (47). It is likely that in our mice, deleting *Gfi1* in the intestinal epithelium resulted in more Neurog3^{+} enteroendocrine cell progenitors, and subsequent loss of heterozygosity of *APC* within this expanded pool of Neurog3^{+} progenitors leads to hyperplastic lesions of endocrine cells, which we observed as CgA^{+} cell clusters. Our finding further suggests that the biological basis for colorectal neuroendocrine tumors (NET) may be distinct from NETs found in other tissues such as small intestine, stomach, and pancreas. This hypothesis is further supported by the observation in the COSMIC database that colorectal NETs primarily bear mutations in *p53, APC*, and *β-catenin*, whereas other gastroentero-pancreatic NETs bear a different mutation profile, including alterations of *MEN1, DAXX*, and *ATRX* (48).

Adenomatous polyposis coli (APC) acts as a central gatekeeper gene in colorectal tumorigenesis. Mutational inactivation of the *APC* gene is found in >80% of human colon tumors (49). C57BL/6L mice carrying the *Min* allele of *APC* (Apc$^{Min/+}$) develop numerous adenomatous polyps due to loss of heterozygosity and are the most widely used mouse model for studying intestinal tumorigenesis (50). However, Apc$^{Min/+}$ mice have limitations for modeling human colorectal cancer, because they develop numerous adenomas predominantly located in the small intestine, whereas in humans sporadic and inherited intestinal cancers arise in the colon and rectum. Moreover, Apc$^{Min/+}$ mice do not develop invasive cancer because they die at an early age do to obstruction caused by tumor burden in the small intestine. Here, we have found that deleting *Gfi1* in the colon using the CDX2-cre transgene in Apc$^{min/+}$ mice produced a larger number of advanced adenomas and carcinomas in the distal colon and rectum at the age of 4 to 5 months. Therefore, these mice provide a valuable model for studying colorectal cancer that overcomes the limitations of developing advanced adenocarcinoma in Apc$^{Min/+}$ mice.

In summary, genetic knockouts in a transgenic mouse model and molecular analyses in human colorectal cancer samples and cell lines support the role of GFI1 as a tumor suppressor. Furthermore, Apc$^{Min/+}$ mice carrying a colon-specific deletion of *Gfi1* develop advanced tumors in the distal colon and rectum, suggesting that Gfi1 is a critical tumor suppressor and driver of malignancy in colorectal cancer. Our findings suggest that GFI1 may have distinct roles in different histologic subtypes of colorectal cancer. Therefore, elucidating the basic mechanisms of GFI1 function, its target genes, and interacting proteins as well as identification of pathways that control *GFI1* expression will help to define rationally targeted therapies for mucinous and nonmucinous colorectal cancer.

Supplementary Material

Refer to Web version on PubMed Central for supplementary material.

Acknowledgments

The authors thank the Texas Medical Center Digestive Disease Center for their support with funding from the NCI (P30DK56338), the Intestinal Stem Cell Consortium with funding from the NIH through grants (U01 DK103168 and U01 DK103168-03S), NIH grants R01 CA142826 (N.F. Shroyer) and F99 CA212433 (Y.-H. Lo). We thank the Integrated Microscopy Core at Baylor College of Medicine for their support with funding from the NIH (NCI-CA125123 and NIDDK-56338-13/15) and CPRIT (RP150578), the Cytometry and Cell Sorting Core at Baylor College of Medicine with funding from the NIH (P30 AI036211, P30 CA125123, and S10 RR024574), the Pathology and Histology Core (HTAP) at Baylor College of Medicine with grant from NCI (NCI-CA125123) and the Dan L. Duncan Cancer Center.

References

1. Siegel RL, Miller KD, Jemal A. Cancer statistics, 2016. CA Cancer J Clin 2016;66:7–30. [PubMed: 26742998]
2. Gonzalez-Pons M, Cruz-Correa M. Colorectal cancer biomarkers: where are we now? Biomed Res Int 2015;2015:149014. [PubMed: 26106599]
3. Bupathi M, Wu C. Biomarkers for immune therapy in colorectal cancer: Mismatchrepair deficiency and others. J Gastrointest Oncol 2016;7: 713–20. [PubMed: 27747085]
4. Fichera A Risk of progression of advanced adenomas to colorectal cancer by age and sex: estimates based on 840,149 screening colonoscopies—Abstractor's comment. Dis Colon Rectum 2008;486–7.
5. Bhagwat AS, Vakoc CR. Targeting transcription factors in cancer. Trends Cancer 2015;1:53–65. [PubMed: 26645049]
6. Karsunky H, Zeng H, Schmidt T, Zevnik B, Kluge R, Schmid KW, et al. Inflammatory reactions and severe neutropenia in mice lacking the transcriptional repressor GFi1. Nat Genet 2002;30:295–300. [PubMed: 11810106]
7. Person RE, Li FQ, Duan Z, Benson KF, Wechsler J, Papadaki HA, et al. Mutations in proto-oncogene GFI1 cause human neutropenia and target ELA2. Nat Genet 2003;34:308–12. [PubMed: 12778173]
8. Zeng H, Yücel R, Kosan C, Klein-Hitpass L, Möröy T. Transcription factor Gfi1 regulates self-renewal and engraftment of hematopoietic stem cells. EMBO J 2004;23:4116–25. [PubMed: 15385956]
9. Hock H, Hamblen MJ, Rooke HM, Schindler JW, Saleque S, Fujiwara Y, et al. Gfi-1 restricts proliferation and preserves functional integrity of haematopoietic stem cells. Nature 2004;431:1002–7. [PubMed: 15457180]
10. Zhu J, Jankovic D, Grinberg A, Guo L, Paul WE. Gfi-1 plays an important role in IL-2-mediated Th2 cell expansion. Proc Natl Acad Sci U S A 2006; 103:18214–9. [PubMed: 17116877]
11. Rathinam C, Klein C. Trancriptional repressor Gfi1 integrates cytokine-receptor signals controlling B-cell differentiation. PLoS One 2007;2:e306. [PubMed: 17375192]
12. Pargmann D, Yücel R, Kosan C, Saba I, Klein-Hitpass L, Schimmer S, et al. Differential impact of the transcriptional repressor Gfi1 on mature CD4+ and CD8+ T lymphocyte function. Eur J Immunol 2007;37:3551–63. [PubMed: 18034420]
13. Gilks CB, Bear SE, Grimes HL, Tsichlis PN. Progression of interleukin-2 (IL-2)-dependent rat T cell lymphoma lines to IL-2-independent growth following activation of a gene (Gfi-1) encoding a novel zinc finger protein. Mol Cell Biol 1993;13:1759–68. [PubMed: 8441411]
14. Bjerknes M, Cheng H. Cell Lineage metastability in Gfi1-deficient mouse intestinal epithelium. Dev Biol 2010;345:49–63. [PubMed: 20599897]
15. Shroyer NF, Wallis D, Venken KJT, Bellen HJ, Zoghbi HY. Gfi1 functions downstream of Math1 to control intestinal secretory cell subtype allocation and differentiation. Genes Dev 2005;19:2412–7. [PubMed: 16230531]
16. Linnoila RI, Jensen-Taubman S, Kazanjian A, Grimes HL. Loss of GFI1 impairs pulmonary neuroendorine cell proliferation, but the neuroendocrine phenotype has limited impact on post-naphthalene airway repair. Lab Investig 2007;87:336–44. [PubMed: 17377622]
17. Kazanjian A, Wallis D, Au N, Nigam R, Venken KJT, Cagle PT, et al. Growth factor independence-1 is expressed in primary human neuroendocrine lung carcinomas and mediates the

differentiation of murine pulmonary neuroendocrine cells. Cancer Res 2004;64:6874–82. [PubMed: 15466176]

18. Dwivedi PP, Anderson PH, Tilley WD, May BK, Morris HA. Role of oncoprotein Growth Factor Independent-1 (GFI1) in repression of 25-hydroxyvitamin D 1alpha-hydroxylase (CYP27B1): A comparative analysis in human prostate cancer and kidney cells. J Steroid Biochem Mol Biol 2007;103:742–6. [PubMed: 17207994]
19. Dwivedi PP, Anderson PH, Omdahl JL, Grimes HL, Morris HA, May BK. Identification of growth factor independent-1 (GFI1) as a repressor of 25-hydroxyvitamin D 1-alpha hydroxylase (CYP27B1) gene expression in human prostate cancer cells. Endocr Relat Cancer 2005;12:351–65. [PubMed: 15947108]
20. Huang M, Hu Z, Chang W, Ou D, Zhou J, Zhang Y. The growth factor independence-1 (Gfi1) is overexpressed in chronic myelogenous Leukemia. Acta Haematol 2009;123:1–5. [PubMed: 19887785]
21. Cancer Genom Atlas. Comprehensive molecular characterization of human colon and rectal cancer. Nature 2012;487:330–7. [PubMed: 22810696]
22. Meerbrey KL, Hu G, Kessler JD, Roarty K, Li MZ, Fang JE, et al. The pINDUCER lentiviral toolkit for inducible RNA interference in vitro and in vivo. Proc Natl Acad Sci U S A 2011;108:3665–70. [PubMed: 21307310]
23. Hinoi T, Akyol A, Theisen BK, Ferguson DO, Greenson JK, Williams BO, et al. Mouse model of colonic adenoma-carcinoma progression based on somatic Apc inactivation. Cancer Res 2007;67:9721–30. [PubMed: 17942902]
24. Klein M, Vignaud JM, Hennequin V, Toussaint B, Bresler L, Plénat F, et al. Increased expression of the vascular endothelial growth factor is a pejorative prognosis marker in papillary thyroid carcinoma. J Clin Endocrinol Metab 2001;86:656–8. [PubMed: 11158026]
25. Williams CS, Zhang B, Smith JJ, Jayagopal A, Barrett CW, Pino C, et al. BVES regulates EMT in human corneal and colon cancer cells and is silenced via promoter methylation in human colorectal carcinoma. J Clin Invest 2011; 121:4056–69. [PubMed: 21911938]
26. Hock H, Hamblen MJ, Rooke HM, Traver D, Bronson RT, Cameron S, et al. Intrinsic requirement for zinc finger transcription factor Gfi-1 in neutrophil differentiation. Immunity 2003;18:109–20. [PubMed: 12530980]
27. Ueo T, Imayoshi I, Kobayashi T, Ohtsuka T, Seno H, Nakase H, et al. The role of Hes genes in intestinal development, homeostasis and tumor formation. Development 2012;139:1071–82. [PubMed: 22318232]
28. Lee TI, Young RA. Transcriptional regulation and its misregulation in disease. Cell 2013;1237–51. [PubMed: 23498934]
29. Avedis K, Eleanore AG, Grimes HL. The growth factor independence-1 transcription factor: New functions and new insights. Crit Rev Oncol Hematol 2006;59:85–97. [PubMed: 16716599]
30. Jen J, Wang Y-C. Zinc finger proteins in cancer progression. J Biomed Sci 2016;23:53. [PubMed: 27411336]
31. Phelan JD, Shroyer NF, Cook T, Gebelein B, Grimes HL. Gfi1-cells and circuits: Unraveling transcriptional networks of development and disease. Curr Opin Hematol 2010;17:300–7. [PubMed: 20571393]
32. Vo BHT, Li C, Morgan MA, Theurillat I, Finkelstein D, Wright S, et al. Inactivation of Ezh2 upregulates Gfi1 and drives aggressive Myc-driven group 3 medulloblastoma. Cell Rep 2017;18:2907–17. [PubMed: 28329683]
33. Xing W, Xiao Y, Lu X, Zhu H, He X, Huang W, et al. GFI1 downregulation promotes inflammation-linked metastasis of colorectal cancer. Cell Death Differ 2017;24:929–43. [PubMed: 28387757]
34. Wassef M, Margueron R. The multiple facets of PRC2 alterations in cancers. J Mol Biol 2017;429:1978–93. [PubMed: 27742591]
35. Wang CG, Ye YJ, Yuan J, Liu FF, Zhang H, Wang S. EZH2 and STAT6 expression profiles are correlated with colorectal cancer stage and prognosis. World J Gastroenterol 2010;16:2421–7. [PubMed: 20480530]

36. Bachmann IM, Halvorsen OJ, Collett K, Stefansson IM, Straume O, Haukaas SA, et al. EZH2 expression is associated with high proliferation rate and aggressive tumor subgroups in cutaneous melanoma and cancers of the endometrium, prostate, and breast. J Clin Oncol 2006;24:268–73. [PubMed: 16330673]
37. Lo YH, Chung E, Li Z, Wan YW, Mahe MM, Chen MS, et al. Transcriptional regulation by ATOH1 and its target SPDEF in the intestine. Cell Mol Gastroenterol Hepatol 2017;3:51–71. [PubMed: 28174757]
38. Bossuyt W, Kazanjian A, De Geest N, Van Kelst S, De Hertogh G, Geboes K, et al. Atonal homolog 1 is a tumor suppressor gene. PLoS Biol 2009;7: 0311–26.
39. Park JS, Huh JW, Park YA, Cho YB, Yun SH, Kim HC, et al. Prognostic comparison between mucinous and nonmucinous adenocarcinoma in colorectal cancer. Medicine (Baltimore) 2015;94:e658. [PubMed: 25881840]
40. Leopoldo S, Lorena B, Cinzia A, Gabriella DC, Angela Luciana B, Renato C, et al. Two subtypes of mucinous adenocarcinoma of the colorectum: clinicopathological and genetic features. Ann Surg Oncol 2008;15: 1429–39. [PubMed: 18301950]
41. Yang L, Cai Y, Zhang J, Hu H, Wenjing W, Wu Z, et al. Colorectal cancer with mucinous component compared to clinicopathological and molecular features as mucinous adenocarcinoma. J Clin Oncol 2017; 35:e15166.
42. Kazama Y, Watanabe T, Kanazawa T, Tada T, Tanaka J, Nagawa H. Mucinous carcinomas of the colon and rectum show higher rates of microsatellite instability and lower rates of chromosomal instability: a study matched for T classification and tumor location. Cancer 2005;103: 2023–9. [PubMed: 15812832]
43. Oberg K, Castellano D. Current knowledge on diagnosis and staging of neuroendocrine tumors. Cancer Metastasis Rev 2011;30:3–7. [PubMed: 21311954]
44. Koh TJ, Dockray GJ, Varro A, Cahill RJ, Dangler CA, Fox JG, et al. Over-expression of glycine-extended gastrin in transgenic mice results in increased colonic proliferation. J Clin Invest 1999;103:1119–26. [PubMed: 10207163]
45. Korinek V, Barker N, Moerer P, Van Donselaar E, Huls G, Peters PJ, et al. Depletion of epithelial stem-cell compartments in the small intestine of mice lacking Tcf-4. Nat Genet 1998;19:379–83. [PubMed: 9697701]
46. Pinto D, Gregorieff A, Begthel H, Clevers H. Canonical Wnt signals are essential for homeostasis of the intestinal epithelium. Genes Dev 2003;17: 1709–13. [PubMed: 12865297]
47. Wang Y, Giel-Moloney M, Rindi G, Leiter AB. Enteroendocrine precursors differentiate independently of Wnt and form serotonin expressing adenomas in response to active beta-catenin. Proc Natl Acad Sci U S A 2007;104: 11328–33. [PubMed: 17592150]
48. Forbes SA, Beare D, Boutselakis H, Bamford S, Bindal N, Tate J, et al. COSMIC: Somatic cancer genetics at high-resolution. Nucleic Acids Res 2017;45:D777–83. [PubMed: 27899578]
49. Kinzler KW, Vogelstein B. Lessons from hereditary colorectal cancer. Cell 1996;87:159–70. [PubMed: 8861899]
50. Moser AR, Pitot HC, Dove WF. A dominant mutation that predisposes to multiple intestinal neoplasia in the mouse. Science 1990;247:322–4. [PubMed: 2296722]

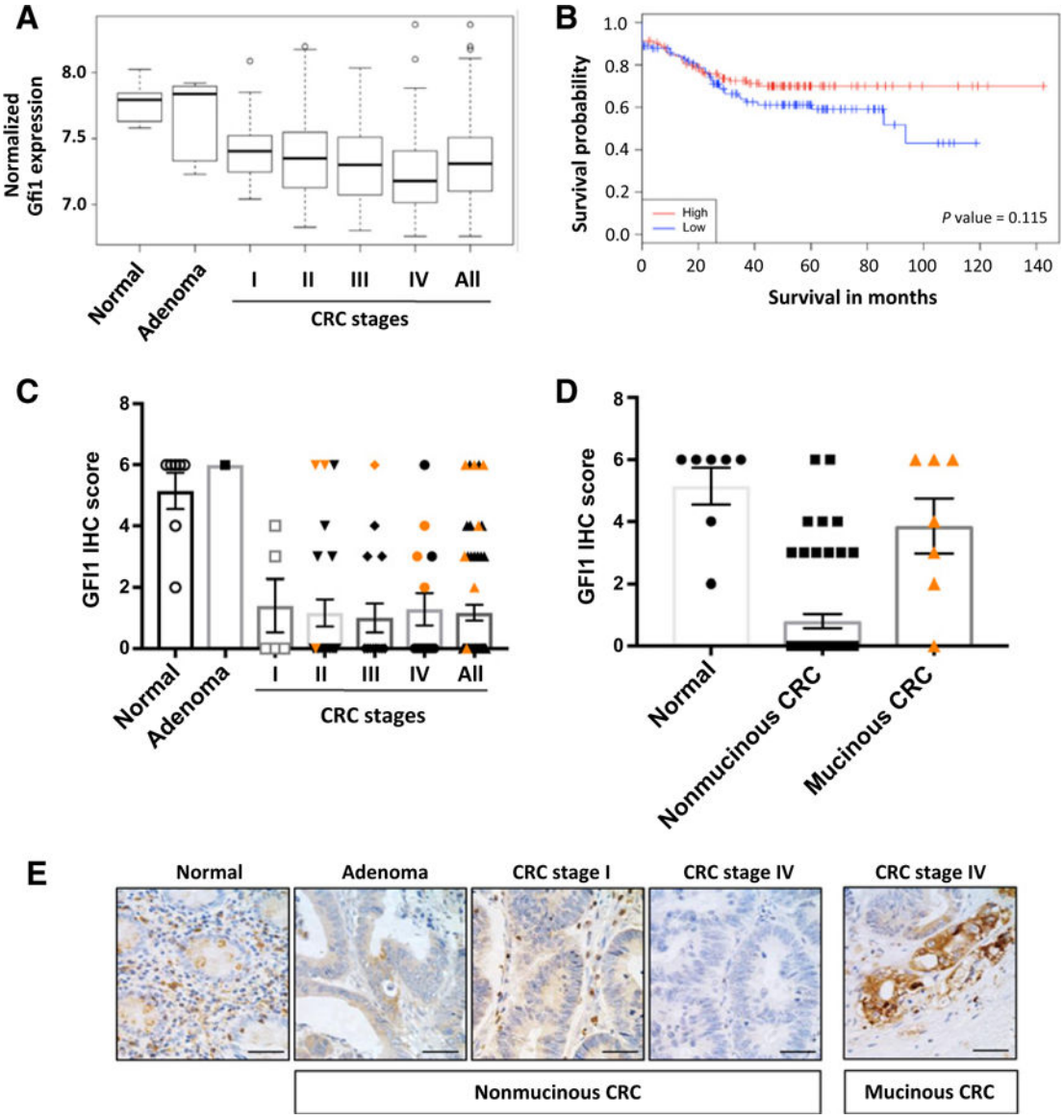

Figure 1.

Expression of GFI1 is decreased in colorectal cancer (CRC). **A,** *GFI1* expression was reduced in colorectal carcinoma compared with benign adenomas and noncancerous tissue (normal vs. all stages, *P* value = 1.267e–5). **B,** Correlation between *GFI1* expression status and prognosis of colorectal cancer patients. (*P* value = 0.115, *N* = 223). **C,** Analysis of Gfi1 expression in colorectal cancer patients. Dot plot showed the distribution of total IHC scores for Gfi1 expression (7, normal samples; 1, adenomas; 5, stage I; 24, stage 2; 16, stage 3; and 14, stage 4; total of 59 colorectal cancer, orange color indicate mucinous colorectal cancer). The bars represent mean and SEM. **D,** Analysis of IHC score for Gfi1 expression in nonmucinous colorectal cancer and mucinous colorectal cancer sample (52, nonmucinous samples; 7 mucinous samples). **E,** Representative Gfi1 IHC images from normal colon, adenocarcinoma, and mucinous colorectal cancer. Scale bars, 50 μm.

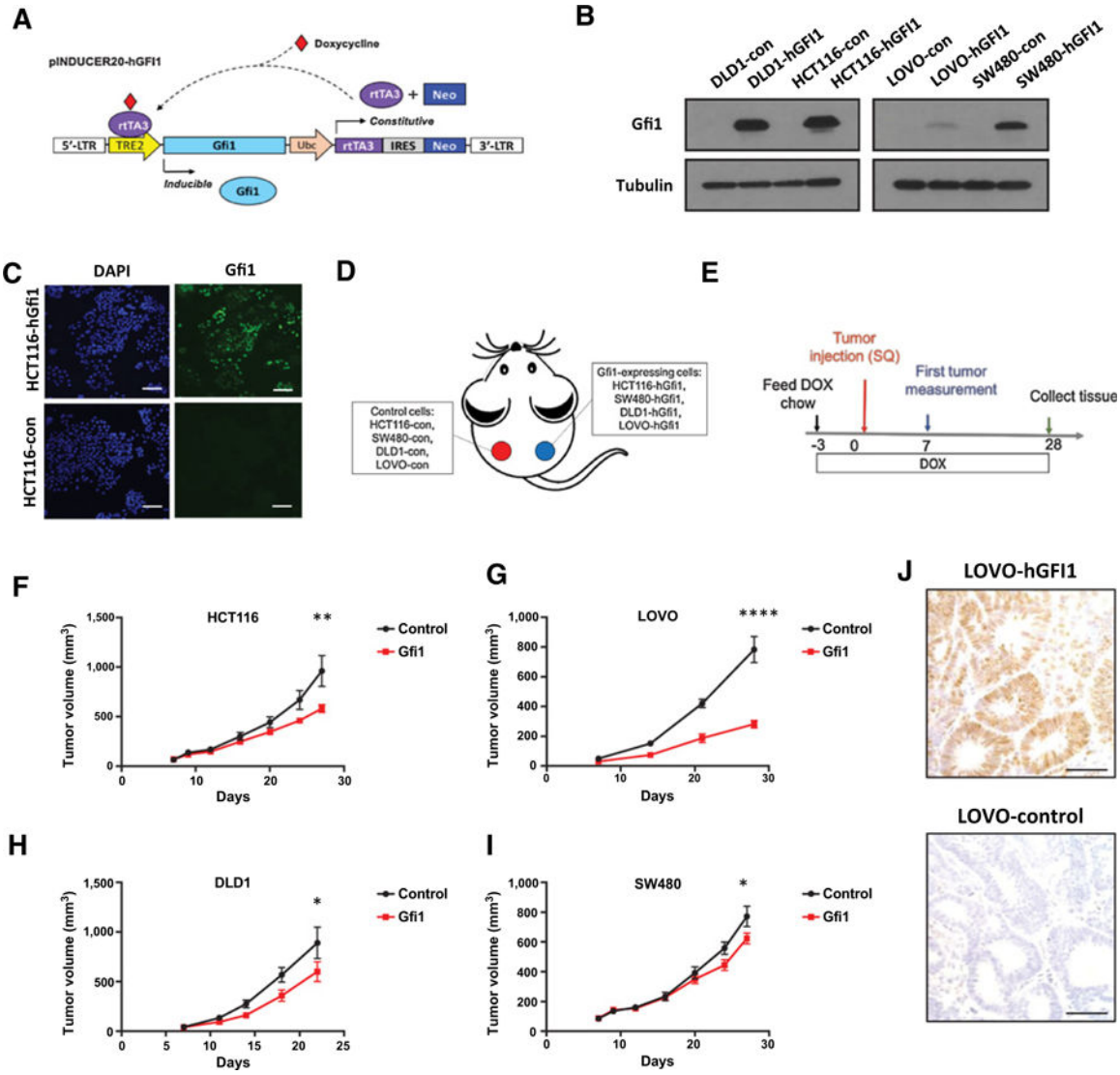

Figure 2.

Reexpression of GFI1 inhibits tumor growth in the subcutaneous tumor model. **A,** Diagram of pINDUCER20-hGFI1. pINDUCER20-hGFI1 encodes a constitutive cassette (rtTA3 and Neo, neomycin resistance) and an inducible transcript (hGFI1). **B,** Immunoblot of GFI1 in colon cancer cell lines expressing pINDUCER20 encoding doxycycline (DOX)-inducible GFI1. Cells were incubated in tetracycline-free serum media in the presence of DOX (1 μg/mL) for 48 hours. **C,** Immunostaining of GFI1 in the colon cancer cell line HCT116 in the presence of DOX for 48 hours. Scale bars, 100 μm. **D,** A diagram of subcutaneous injection of GFI1-expressing and control colorectal cancer cell lines in mice is shown. **E,** Scheme of tumor injection, GFI1 induction, and tissue collection is shown. **F,** Growth of subcutaneous HCT116 colon tumors ($n = 10$ mice per group). **G,** Growth of subcutaneous LOVO colon tumors ($n = 10$ mice per group). **H,** Growth of subcutaneous DLD1 colon tumors ($n = 8$ mice per group). **I,** Growth of subcutaneous SW480 colon tumors ($n = 8$ mice per group). *, $P < 0.05$; **, $P < 0.01$; ****, $P < 0.0001$. Each point represents mean tumor

volume ± SEM. Data are representative of 2 independent experiments. **J,** Immunostaining of GFI1 in LOVO cell–derived xenograft after DOX treatment. Scale bars, 50 μm.

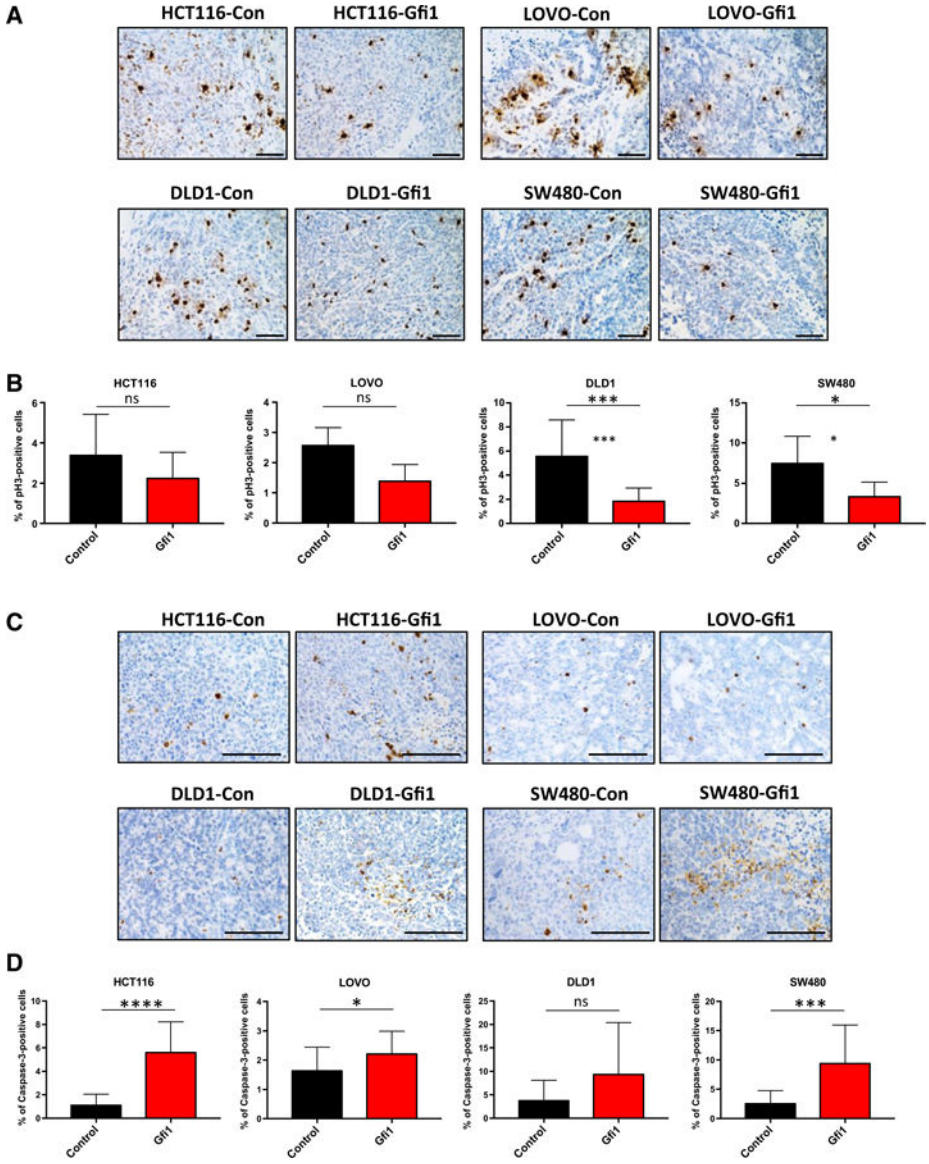

Figure 3.

Reexpression of Gfi1 inhibits cell proliferation and promotes cell apoptosis in subcutaneous xenografts. **A,** Immunostaining of phospho-histone3 (pH3) showing proliferative cells in human colorectal cancer xenografts. Scare bar: 50 μm. **B,** Quantification of positive pH3 staining per field from 5 different fields of each xenograft ($n = 3$ xenografts per group). **C,** Immunostaining of caspase-3 showing apoptotic cells in human colorectal cancer xenografts. **D,** Quantification of caspase-3 staining per field from 5 different fields of each xenograft ($n = 3$ xenografts per group). Scare bar, 50 μm. *, $P < 0.05$; ***, $P < 0.001$; ****, $P < 0.001$; ns, nonsignificant. Bars, SD.

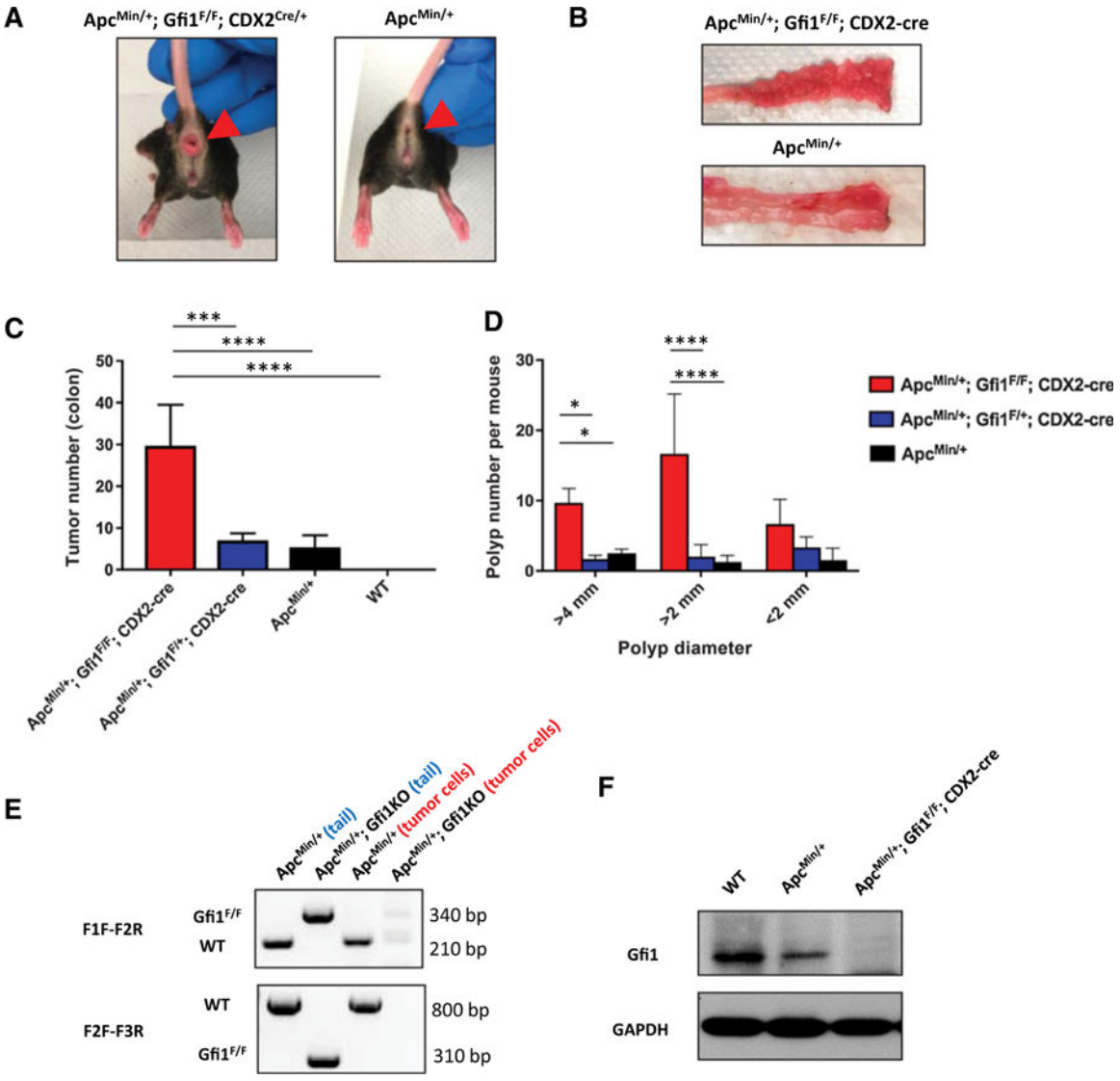

Figure 4.

Gfi1 loss leads to increased tumor burden in the colon of $Apc^{Min/+}$ mice. Representative photographs of rectum (**A**) and longitudinally opened distal colon (**B**) from $Apc^{Min/+}$; $Gfi1^{F/F}$; CDX2-cre and $Apc^{Min/+}$; $Gfi1^{wt}$; $CDX2^{wt}$ ($Apc^{Min/+}$). Analysis of polyps in the colon, (**C**) number of polyps per mouse; (**D**) diameter of polyps in $Apc^{Min/+}$; $Gfi1^{F/F}$; CDX2-cre ($n = 3$ mice), $Apc^{Min/+}$; $Gfi1^{F/+}$; CDX2-cre ($n = 3$ mice), $Apc^{Min/+}$ ($n = 5$ mice), wild-type, WT ($n = 5$ mice). Error bars, SD. **E,** A PCR-based assay identified the $Gfi1^{F/F}$ and Gfi1wt alleles in mouse tails and tumor cells from $Apc^{Min/+}$; $Gfi1^{F/F}$; CDX2-cre ($Apc^{Min/+}$; Gfi1 KO) and $Apc^{Min/+}$ mouse. **F,** Immunoblotting assay showed Gfi1 expression was lost in the colon in $Apc^{Min/+}$; $Gfi1^{F/F}$; CDX2-cre mouse compared with the control mice. *, $P < 0.05$; ***, $P < 0.001$; ****, $P < 0.0001$.

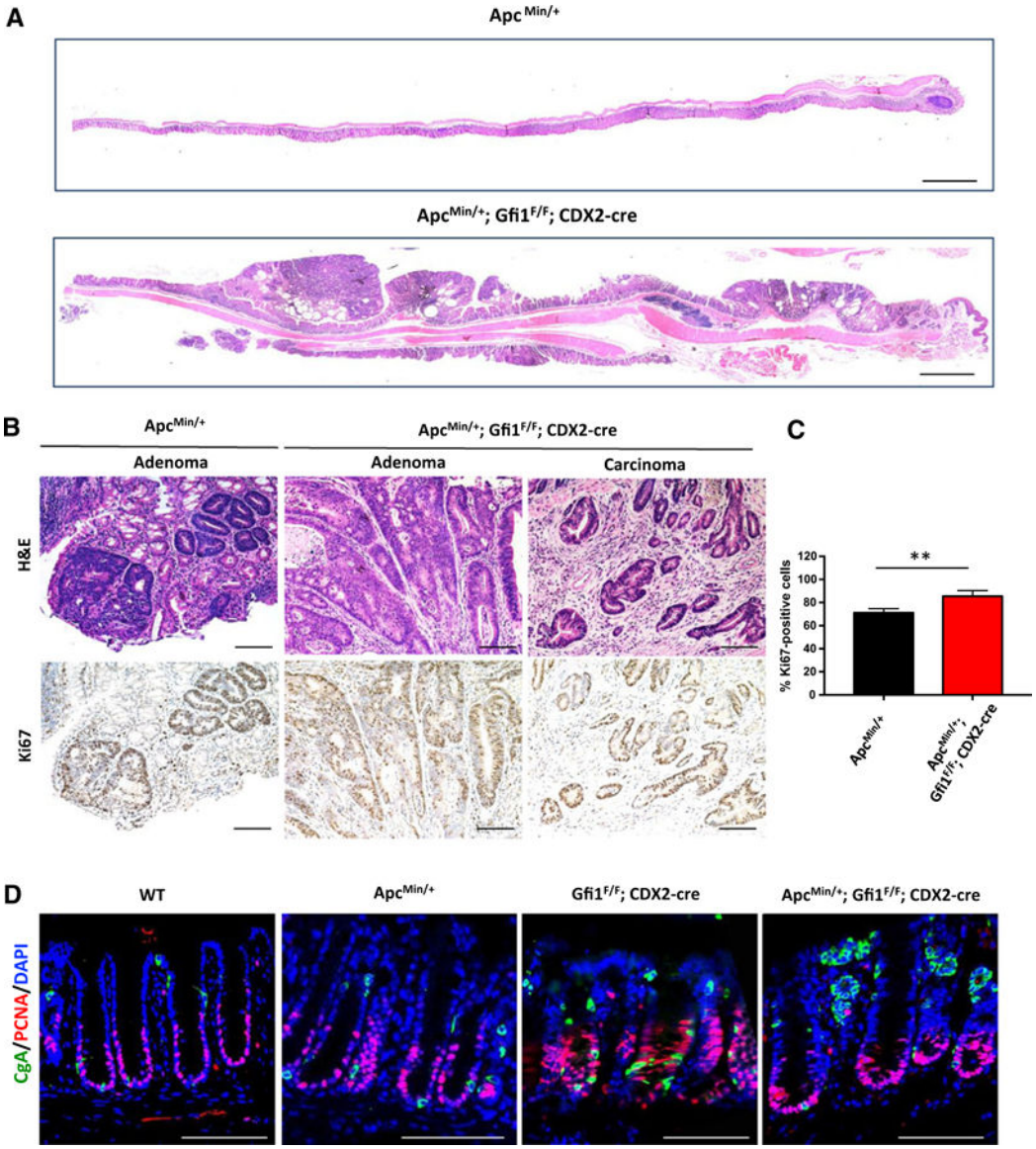

Figure 5.

Histologic analysis of Gfi1 knockout tumors. **A,** Representative H&E histopathology of tumors from $Apc^{Min/+}$; $Gfi1^{F/F}$; CDX2-cre and $Apc^{Min/+}$ mouse. GFI1 knockout mice showed a dramatic increase in the number of adenomas and advanced carcinomas. Scale bar, 1,000 μm. **B,** Histologic images of highly proliferative adenomas and carcinomas from $Apc^{Min/+}$; $Gfi1^{F/F}$; CDX2-cre mouse and adenomas from control $Apc^{Min/+}$ mouse. Scale bar, 100 μm. **C,** Quantification of Ki67-positive cells in adenomas in $Apc^{Min/+}$; $Gfi1^{F/F}$; CDX2-cre and $Apc^{Min/+}$ mice. **D,** Immunostaining of CgA and PCNA in Gfi1 knockout and control mice. Fluorescent images showed enteroendocrine cells (CgA^+) were increased in Gfi1 knockout ($Gfi1^{F/F}$; CDX2-cre) mice. In $Apc^{Min/+}$; $Gfi1^{F/F}$; CDX2-cre mouse, we found hyperplastic lesions with enteroendocrine cell features (CgA^+, green) scattered throughout mucosal layer (right). Proliferative cells were analyzed by PCNA staining. Images showed

CgA^+ clusters were not in proliferation. Green: CgA; Red: PCNA; Blue: DAPI. Scale bars, 100 μm. **, $P < 0.01$.